

Defects in single-crystal silicon induced by hydrogenation

N. M. Johnson, F. A. Ponce, R. A. Street, and R. J. Nemanich*

Xerox Palo Alto Research Center, Palo Alto, California 94304

(Received 16 December 1986)

It is demonstrated that hydrogenation *induces* microdefects and electronic deep levels in single-crystal silicon, which are *unrelated* to either plasma or radiation damage. After hydrogenation of either *n*-type or *p*-type silicon, transmission electron microscopy reveals defects that can be described as hydrogen-stabilized platelets or microcracks which appear within 0.1 μm of the exposed surface and are predominantly oriented along $\{111\}$ crystallographic planes. These defects correlate with high concentrations of hydrogen or deuterium as measured by secondary-ion mass spectrometry and with the appearance of Si—H bonds as revealed by Raman spectroscopy. The concomitant introduction of electrically active gap states is demonstrated with both photoluminescence spectroscopy (PL) and deep-level transient spectroscopy (DLTS). In PL several H-induced radiative transitions are observed, with the dominant peak at 0.98 eV, which had previously been ascribed to plasma damage. In *n*-type Schottky diodes, DLTS detects two H-induced levels with thermal activation energies for electron emission of approximately 0.06 and 0.51 eV. These defects are detected at depths greater than the surface layer, are in low concentrations ($< 10^{13} \text{ cm}^{-3}$), are acceptorlike, and anneal with an activation energy of ~ 0.3 eV.

Current interest in the properties of hydrogen in semiconductors is primarily stimulated by its ability to passivate both shallow-level dopants and deep-level defects at moderate temperatures (e.g., $\leq 300^\circ\text{C}$). Hydrogen is most commonly introduced by exposure to a plasma discharge, and passivation involves the removal of energy levels from the band gap as a consequence of hydrogen chemical bonding. Recent examples of this phenomenon are passivation of shallow-level acceptor and donor dopants in silicon¹⁻³ and gallium arsenide^{4,5} and passivation of oxygen-related thermal donor (deep-level) defects in silicon.⁶ Direct exposure to a plasma, such as occurs in reactive-ion etching, also introduces damage due to charge-particle bombardment.⁷ Hydrogen can interact with this damage to form H-related defects with levels in the band gap.^{8,9} Defect complexes involving hydrogen also appear in crystals grown in a hydrogen atmosphere, which is inherently a high-temperature process (e.g., 938°C for Ge).¹⁰ Silicon grown in a hydrogen atmosphere contains optically active complexes; however, ionizing radiation is required to produce H-related deep levels.¹¹ In this paper it is demonstrated that hydrogen, diffused into single-crystal silicon at moderate temperatures, *generates* extended and electrically active defects that are *unrelated* to either plasma or radiation damage. The results identify the cause of the hydrogen-rich surface layer which has been previously ascribed to the formation of molecular hydrogen. In addition, it is proposed that the defect luminescence previously observed only in plasma-etched silicon is H induced rather than due to damage or carbon contamination from the plasma.

Hydrogenation was performed by exposing specimens of silicon to monatomic hydrogen or deuterium from a gas discharge. The microwave plasma was operated at 70 W and at a pressure of 2 Torr, which consisted of 1.8 Torr of H_2 or D_2 and 0.2 Torr of O_2 . The role of oxygen in a hydrogen plasma is described elsewhere.¹² Specimens were

mounted on a heater stage that was located downstream from the plasma, with baffles for optical isolation. This arrangement eliminates the damage which results from direct immersion in the plasma. Sample location within the heater chamber was also adjusted so that the sample surface temperature during hydrogenation did not exceed the heater stage temperature by more than 10°C (at 150°C). Specifications of the silicon wafers and processing are described below in connection with the different measurement techniques.

The depth profile of hydrogen in silicon can be determined by secondary-ion mass spectrometry (SIMS). For this purpose deuterium is used as a readily identifiable isotope of low natural abundance which duplicates the chemistry of hydrogen and is detectable with high sensitivity by SIMS.^{12,13} The depth profile has been shown to depend on electrical-conductivity type and dopant concentration, as well as on deuteration conditions.^{2,3,12} The dependence on conductivity type is illustrated in Fig. 1 with depth profiles of deuterium for specimens of silicon that were deuterated at 150°C for 60 min. The starting material was doped in the melt with either phosphorus or boron to a uniform concentration of approximately $1 \times 10^{17} \text{ cm}^{-3}$. Of primary interest in the present study is the first 0.1 μm of the depth profiles. In both samples the D density decreases precipitously with depth within this region, with the extrapolated surface density largest in the *n*-type specimen where it approaches $1 \times 10^{20} \text{ cm}^{-3}$. Previous studies have offered the plausible suggestion that this surface peak arises from recombination of fast-diffusing monatomic hydrogen to form interstitial molecular hydrogen which is essentially immobile at moderate temperatures.^{12,14}

Transmission electron microscopy (TEM) reveals the appearance after hydrogenation of planar microdefects within 0.1 μm of the silicon surface. This is demonstrated in Fig. 2 with cross-sectional TEM micrographs, viewed in the $\langle 110 \rangle$ projection, of defects in the near-surface region

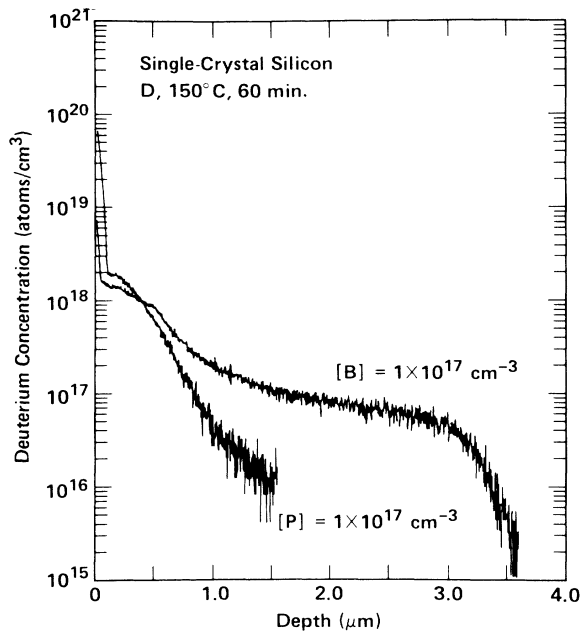


FIG. 1. Depth profiles of deuterium in *n*-type (phosphorus-doped) and *p*-type (boron-doped) silicon after deuteration (150°C, 60 min).

after deuteration of *n*-type silicon. The starting material and deuteration conditions were the same as those that produced the D depth profile in the *n*-type sample in Fig. 1. The bright-field image in Fig. 2(a) reveals an average density of $\sim 7 \times 10^{16}$ microdefects per cm^3 within ~ 70 nm of the surface. No defects were detectable in unhydrogenated specimens. At high magnification [Fig. 2(b)] it can be discerned that the platelets are oriented in $\{111\}$ crystallographic planes; in some samples (e.g., hydrogenated n^+ silicon) $\{100\}$ platelets have also been observed. The high-resolution lattice image of a $\{111\}$ platelet shown in Fig. 2(c) reveals that the platelets are not due to dislocations since a Burgers circuit indicates no net displacement in the lattice. Similarly, there is no evidence that the platelets consist of either interstitial or vacancy loops, since contrast typical of stacking faults¹⁵ was not observed. The platelets appear to be microcracks in which the separation between two adjacent planes of silicon atoms over a finite area (nominal diameter of 3 to 12 nm) is increased due to the slight displacement of silicon atoms from their substitutional lattice sites. From the effect of dopant type and concentration, it was observed that the density of platelets is proportional to the near-surface concentration of D. For example, in the samples examined in Fig. 1 the platelet density was of the order of a factor of 100 less in the *p*-type as compared to the *n*-type specimens. In addition, partial removal of D by a vacuum anneal (350°C, 60 min) was accompanied by a decrease in the platelet density. These observations strongly suggest that the platelets are not only induced by hydrogenation but are also stabilized by the direct involvement of hydrogen in the defect structure.

Direct support for the idea that the platelets are hydro-

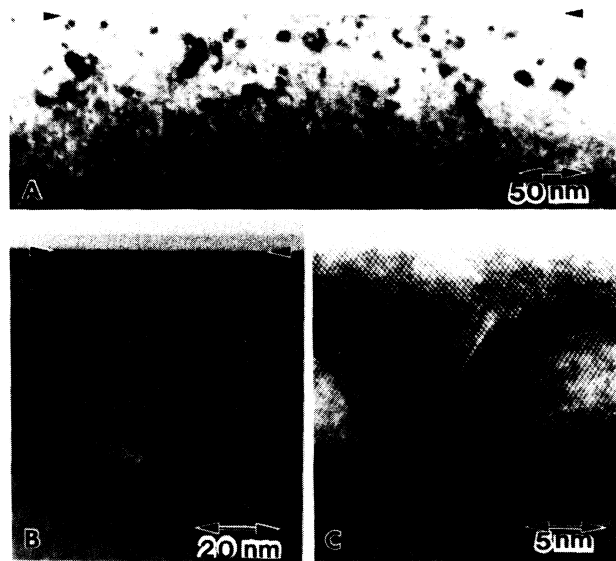


FIG. 2. Cross-sectional TEM micrographs, viewed in a $\langle 110 \rangle$ projection of defects in the near-surface region of (100) -oriented silicon after deuteration (150°C, 60 min): A, bright-field image showing large density of microdefects in proximity of surface; B, high magnification of surface region; and C, high-resolution lattice image.

gen stabilized is provided by Raman spectroscopy. Spectra are shown in Fig. 3 for specimens of *n*-type Si ($[P] = 1 \times 10^{17} \text{ cm}^{-3}$) that were hydrogenated at 156°C for 30 min. The spectra have been expanded several times to display the weak features. All the features appearing at less than 1500 cm^{-1} are due to Si lattice vibrations; for example, the peaks at ~ 520 , 980, and 1470 cm^{-1} are the zone-center optical phonon, the two-phonon overtone of

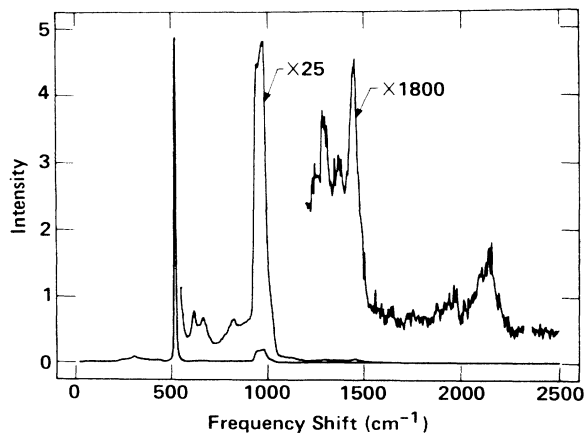


FIG. 3. The Raman spectrum for (100) -oriented silicon after hydrogenation (156°C, 30 min). The spectra are expanded several times to display the spectral features of the weak H-induced modes at ~ 1960 and 2100 cm^{-1} .

the optical phonon branch, and the three-phonon overtone, respectively. The spectral features centered at 1960 and 2100 cm^{-1} are attributed to H incorporated in the Si lattice. Indeed, the 2100- cm^{-1} mode is characteristic of Si—H bonding and displayed the expected isotopic frequency shift in deuterated samples.¹⁶ An extended scan to 5000 cm^{-1} showed no evidence of hydrogen molecules in the lattice; however, the Raman cross section of H_2 in Si has not been established. The intensities of the two H-induced modes are approximately a factor of 7000 weaker than those for the Si lattice modes. This implies an average H concentration of the order of $7 \times 10^{18} \text{ cm}^{-3}$ in the near-surface layer, which is consistent with SIMS results (e.g., see Fig. 1). If the platelets are a consequence of the coordinated formation of Si—H bonds, perhaps driven by strain, then for an average diameter of 7 nm each platelet would contain roughly 400 Si—H bonds. The platelet density then yields a total estimated H concentration that is consistent with the proposal that a large proportion of the Raman-detected H is incorporated in the near-surface platelets.

The generation of platelets during hydrogenation is accompanied by the introduction of electronic deep levels in the silicon band gap. This is demonstrated in Fig. 4 with

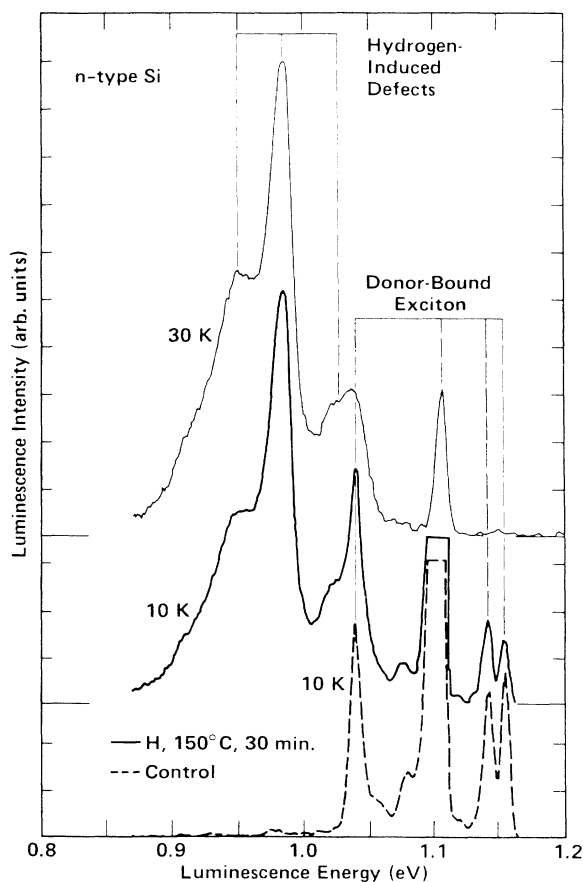


FIG. 4. Luminescence spectra for *n*-type ($8\text{-}\Omega\text{-cm}$) silicon before (control) and after hydrogenation (150°C , 30 min). The spectra are offset vertically to ease inspection.

luminescence spectra, recorded at different temperatures, for *n*-type silicon before (control) and after hydrogenation (150°C , 30 min). In the control sample the spectrum is dominated by the commonly observed luminescence peaks arising from annihilation of donor-bound excitons.¹⁷ After hydrogenation the spectrum contains several new transitions with the most prominent peaks at approximately 0.95, 0.98, and 1.03 eV. From the temperature dependence of the luminescence intensities it appears that the 1.03 and 0.98 eV peaks are related as the zero-phonon line and a TO-phonon replica, respectively, for radiative recombination at a specific defect, while the peak or shoulder at 0.95 eV is due to a different recombination site.

The H-induced luminescence may be related to platelet formation. The magnitude of the luminescence intensities is more consistent with the platelet density than with the deep-level densities detected by DLTS and discussed below. In addition, the luminescence intensity was found to be greatly attenuated in *p*-type as compared to *n*-type samples of comparable doping concentration and identical hydrogenation conditions. On the other hand, the absence of a clearly-identifiable isotopic effect suggests that the radiative recombination site may not directly incorporate hydrogen. A comparison of the annealing kinetics of the H-induced luminescence and the platelets is currently in progress. Finally, defect luminescence spectra similar to those shown in Fig. 4 have been reported and ascribed to carbon contamination and damage during plasma etching of silicon.¹⁸ The present study establishes that the defect luminescence characteristic of plasma-etched silicon need not arise from either displacement damage or impurities other than hydrogen from the plasma.

Hydrogen-induced gap states were also detected by deep-level transient spectroscopy (DLTS); the DLTS technique is reviewed in Ref. 19. These defects cannot be directly associated with the H-induced platelets since the spatial observation window for deep-level detection did not overlap with the surface layer. Schottky-barrier diodes were fabricated on *n*-type ($[P] \approx 7 \times 10^{15} \text{ cm}^{-3}$) silicon by vacuum-depositing Pt electrodes on the polished silicon surface after hydrogenation; the wafers had previously received Ohmic back contacts. A DLTS spectrum for a diode that was hydrogenated at 150°C for 50 min is shown in Fig. 5. From an Arrhenius analysis of the emission rates for the two peaks, the activation energies for thermal emission of electrons were found to be $55 \pm 5 \text{ meV}$ and $0.51 \pm 0.01 \text{ eV}$. In unhydrogenated diodes no peaks appeared at the same DLTS sensitivity. From the diode parameters and DLTS measurement conditions, the two deep levels were found to have essentially the same average density of $7.5 \times 10^{12} \text{ cm}^{-3}$ with spatial observation windows of $0.45 \rightarrow 1.13 \mu\text{m}$ for the 0.06-eV level and $0.11 \rightarrow 0.84 \mu\text{m}$ for the 0.51-eV level. Neither level displayed a significant dependence on applied electric field. The absence of a Poole-Frenkel effect²⁰ suggests that both defects are acceptorlike. Finally, it was observed that the density of both levels significantly decreased over a period of weeks at room temperature; the annealing kinetics of the 0.51-eV level yielded a thermal activation energy of approximately 0.3 eV. These deep-level defects may arise from the formation of a weak chemical bond between in-

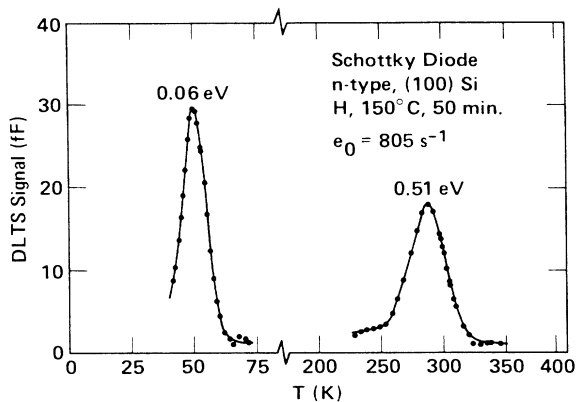


FIG. 5. DLTS spectrum for a Schottky diode on *n*-type silicon ($[P] \approx 7 \times 10^{15} \text{ cm}^{-3}$) after hydrogenation (150°C , 50 min). The emission rate window e_0 was obtained with delay times of 0.5 and 2.5 ms.

terstitial hydrogen and either a Si atom or an unidentified impurity.

The results presented above establish that diffusing hydrogen into single-crystal silicon generates microdefects and electronic gap states, which are unrelated to either plasma or radiation damage. With reference to the D depth profiles in Fig. 1, the near-surface peak is a manifestation of the nucleation and growth of platelets that are stabilized by the formation of Si—H bonds. Platelet nu-

cleation may involve interstitial molecular hydrogen or passivated dopants. The gap states detected by luminescence may be due to strain-induced defects that are associated with platelet formation. Beyond the surface layer, the D concentration decreases gradually with distance into the bulk. Within this subsurface zone, deep-level defects are generated by diffusing hydrogen. However, the concentration of these defects is several orders of magnitude smaller than either the D concentration or typical dopant densities. The concentration is, therefore, too small for these defects to be a significant contributing factor (e.g., via compensation) in hydrogen passivation of *n*-type or *p*-type dopants, which has been shown^{1,2,6} to extend to depths greater than the immediate surface layer. While it is no longer justifiable to hypothesize the predominance of interstitial molecular hydrogen in the H-rich surface layer, electrically inactive H_2 may be the dominant form of hydrogen over that portion of the subsurface zone in which the H concentration exceeds the dopant density (see Fig. 1). Finally, carrier transport properties within the H-rich surface layer should be affected by the significant concentrations of electrically active defects.

The authors are pleased to acknowledge stimulating discussions with C. Herring and D. J. Chadi. The authors also thank J. Walker, J. Tramontana, and G. Anderson for technical support. The SIMS measurements were performed at Charles Evans and Associates (Redwood City, California).

*Present address: Department of Physics, North Carolina State University, Raleigh, NC 27650-8202.

¹J. I. Pankove, D. E. Carlson, J. E. Berkeyheiser, and R. O. Wance, *Phys. Rev. Lett.* **51**, 2224 (1983).

²N. M. Johnson, *Phys. Rev. B* **31**, 5525 (1985).

³N. M. Johnson, C. Herring, and D. J. Chadi, *Phys. Rev. Lett.* **56**, 769 (1986).

⁴J. Chevallier, W. C. Dautremont-Smith, C. W. Tu, and S. J. Pearton, *Appl. Phys. Lett.* **47**, 108 (1985).

⁵N. M. Johnson, R. D. Burnham, R. A. Street, and R. L. Thornton, *Phys. Rev. B* **33**, 1102 (1986).

⁶N. M. Johnson and S. K. Hahn, *Appl. Phys. Lett.* **48**, 709 (1986).

⁷G. S. Oehrlein, *J. Appl. Phys.* **59**, 3053 (1986).

⁸M. O. Watanabe, M. Taguchi, K. Kanzaki, and Y. Zohta, *Jpn. J. Appl. Phys.* **22**, 281 (1983).

⁹J. M. Hwang, D. K. Schroder, and W. J. Biter, *J. Appl. Phys.* **57**, 5275 (1985).

¹⁰E. E. Haller, W. L. Hansen, and F. S. Goulding, *Adv. Phys.* **30**, 93 (1981).

¹¹G. G. Qin, Y. C. Du, J. Wu, and X. C. Yao, in *Proceedings of the Fourteenth International Conference on Defects in Semiconductors*, edited by H. J. von Bardeleben, Materials Science Forum (Trans Tech, Switzerland, 1986), Vols. 10–12, pp. 563–572.

¹²N. M. Johnson and M. D. Moyer, *Appl. Phys. Lett.* **46**, 787 (1985).

¹³N. M. Johnson, D. K. Biegelsen, and M. D. Moyer, *Appl. Phys. Lett.* **40**, 882 (1982).

¹⁴R. N. Hall, *J. Electron. Mater.* **14a**, 759 (1985).

¹⁵F. A. Ponce, T. Yamashita, R. H. Bube, and R. Sinclair, in *Defects in Semiconductors*, edited by J. Narayan and T. Y. Tan, Materials Research Society Symposia Proceedings, 2 (North-Holland, Amsterdam, 1981), p. 503.

¹⁶G. Lucovsky, R. J. Nemanich, and J. C. Knights, *Phys. Rev. B* **19**, 2064 (1979).

¹⁷P. J. Dean, J. R. Hayes, and W. F. Flood, *Phys. Rev.* **161**, 711 (1967).

¹⁸I. W. Wu, R. H. Bruce, J. C. Mikkelsen, Jr., R. A. Street, T. Y. Huang, and D. Braun, in *Plasma Processing*, edited by J. W. Coburn, R. A. Gottscho, and D. W. Hess, Materials Research Society Symposia Proceedings, 68 (MRS, Pittsburgh, 1986), p. 381.

¹⁹N. M. Johnson, in *Materials Characterization*, edited by N. W. Cheung and M.-A. Nicolet, Materials Research Society Symposia Proceedings, 69 (MRS, Pittsburgh, 1986), p. 75.

²⁰J. Frenkel, *Phys. Rev.* **54**, 647 (1939).

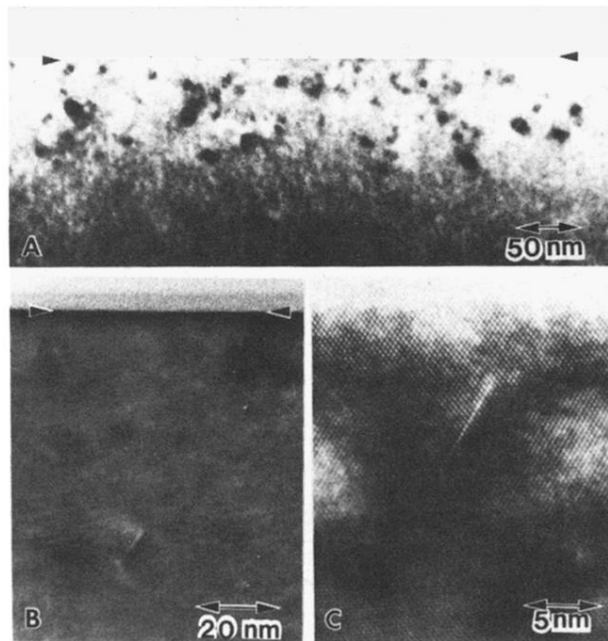


FIG. 2. Cross-sectional TEM micrographs, viewed in a $\langle 110 \rangle$ projection of defects in the near-surface region of (100)-oriented silicon after deuteration (150°C , 60 min): A, bright-field image showing large density of microdefects in proximity of surface; B, high magnification of surface region; and C, high-resolution lattice image.